Inverse Problems, Design and Optimization Symposium
Rio de Janeiro, Brazil, 2004

PERFORMANCE ANALYSIS OF ITERATIVE RECONSTRUCTION ALGORITHMS IN ELECTRICAL CAPACITANCE TOMOGRAPHY

Daniel Watzenig and Bernhard Brandstätter
Christian Doppler Laboratory for Automotive Measurement Research
located at the
Institute of Electrical Measurement and Measurement Signal Processing
Graz University of Technology, Austria
watzenig@emt.tugraz.at and brand@ieee.org

ABSTRACT

In this paper we analyze the different performances of iterative algorithms for a capacitance tomography problem. In particular, the Gauss-Newton scheme using the approximate Hessian is compared with the nonlinear conjugate gradients method. Several aspects like convergence rate, computational cost, amount of the remaining solution norm and image quality have to be taken into account. The image reconstructions are based on real measurement data provided the developed prototype sensor developed at our department.

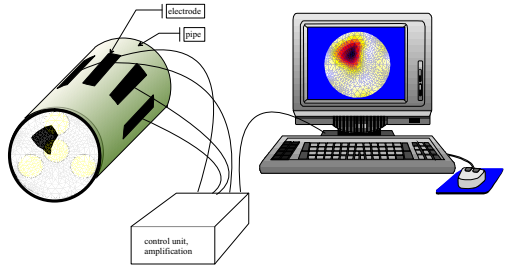

Figure 1: The permittivity distribution inside a closed object (pipe) is reconstructed by means of voltage measurements at electrodes outside the object.

INTRODUCTION

The reconstruction of the material distribution inside a closed pipe is often required for controlling industrial processes. A detailed description of the method, i. e. calculation of the forward problem and the Jacobian is given in [1]. Due to the illposedness of the problem a regularization term has to be introduced. A novel method to adapt this regularization term iteratively is introduced. In order to fulfill the requirements of real-time needs and high image qualities the choice of the reconstruction algorithm plays an important role for the reconstruction task.

For electrical capacitance tomography we search for the relative permittivity distribution ε_r inside a closed object, like for instance, a pipe by measuring the resulting electrical potentials at floating electrodes surrounding the pipe. Other electrodes at the pipe's surface serve as active electrodes, i. e. electrodes on which a known potential is prescribed (fig. 1).

For the forward problem solution (determination of the potentials at floating electrodes from a given permittivity distribution and a given set of active electrodes (with a prescribed potential)) the governing equations to be solved are Gauss' and Faraday's law for the static case leading to a Poisson equation in the interior of the pipe: $\nabla\left(\varepsilon\left(\nabla V\right)\right) = 0$, where ε is the spatial dependent electric permittivity ($\varepsilon = \varepsilon_0\varepsilon_r$, where ε_0 is the permittivity of air and ε_r is the dimensionless relative permittivity) and V is the electric scalar potential. Dirichlet boundary conditions apply at the position of the electrodes, while homogeneous Neumann boundary conditions apply elsewhere on the boundary. The forward problem is solved by means of a finite element approach. Thus, the domain of interest is discretized by linear triangular finite elements with constant permittivity values. The number of finite elements inside the pipe equals the number of degrees of freedom of the inverse problem.

For the inverse problem the permittivities of fi-

nite elements inside the pipe are varied until the difference of the output voltage of the finite element model and the measured voltages is minimal.

For obtaining a reasonable solution for a regularized reconstruction problem, it is necessary to find a good choice for the regularization parameter. In our case we use a discrete Laplace operator for the regularization matrix in order to incorporate some smoothness assumption on the solution.

The inverse problem can be formulated as follows:

$$\varepsilon_r^* = \arg\min_{\varepsilon_r} \left\{ \|V_m - V_0\|_2^2 + \alpha \|L\varepsilon_r\|_2^2 \right\}, \quad (1)$$

where ε_r^* is the solution vector in the optimal point, V_0 is a vector of measured potentials, L is the regularization matrix and α is a regularization parameter.

EXPERIMENTAL SETUP

In fig. 2, a block diagram of the experimental setup is shown. The sensor head consists of 16 electrodes that are arranged on the outer face of a non-conducting pipe. The shielding of the electrodes is not shown in figure 1 for reasons of clarity. Each electrode can be used as a transmitting electrode (excited by a 10.7 MHz rectangular signal) or as a receiving electrode (measuring the mean electric scalar potential of the electrode).

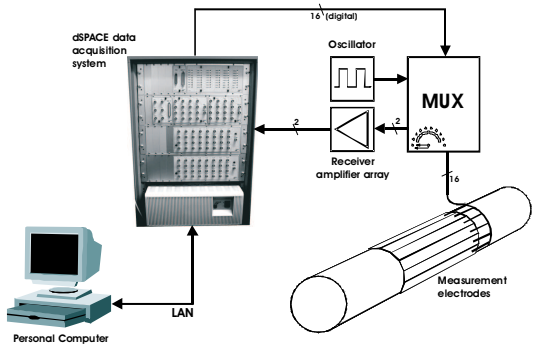

Figure 2: Measurement setup used for ECT measurements: A ring of 16 measurement electrodes is arranged around the tube; the switching circuitry is used to change the operating mode of each electrode (transmit or receive); all needed control signals are provided by the dSPACE system that is connected to a personal computer via local area network.

To simplify the development of the circuitry, the necessary analog/digital conversion is performed by a dSPACE data acquisition system after a pre-amplification step in the sensor front-end. The dSPACE system is a standalone data acquisition and control system, consisting of several modules and controlled by a PowerPC PPC750 CPU. For the task of analog/digital conversion, a dSPACE DS2003 multi-channel A/D converter module is used. This module is operated at a sampling rate of 10 kHz. An additional module, the dSPACE DS4001 timer board, is utilized to generate the control signals for the electronic circuitry. The whole system is programmed using MATLAB/ Simulink running on a Personal Computer connected to the dSPACE system via Local Area Network. To increase data acquisition speed, the core routines are programmed in C and compiled to run on the PPC750 CPU of the dSPACE system.

To overcome the problem of static charge and to decrease the sensitivity to external noise sources, a carrier frequency principle is adopted for the electronic circuitry design. The transmitting electrodes are excited by a 10.7 MHz rectangular signal of selectable polarity. This waveform is chosen since the generation of a rectangular signal with defined amplitude can be easily achieved. In the receiving circuitry, a small-bandwidth ceramic filter is used to extract only the fundamental wave. The main printed circuit board (PCB), containing the signal generation circuitry, the second signal amplification stage and the rectifier circuit, is shaped as two halves of an annulus, and arranged around the pipe to be examined. The first-stage amplifiers are located on 16 small printed circuit boards (one for each electrode) that are plugged onto the main board

THEORETICAL BACKGROUND

For reconstruction problems, where the model states may vary in a wide range, like for Capacitance Tomography, where permittivity values to be reconstructed may be the ones of water (ε_r=80), oil (ε_r=2-3) or air (ε_r=1), the value for the reconstruction parameter is depending on the materials involved (a reconstruction parameter that works for oil and air gives very wrong results for water and oil). Hence an adaptive way of choosing the regularization parameter has to be found.

A method of adapting the regularization parameter was found by our group [5]. For iteration t the

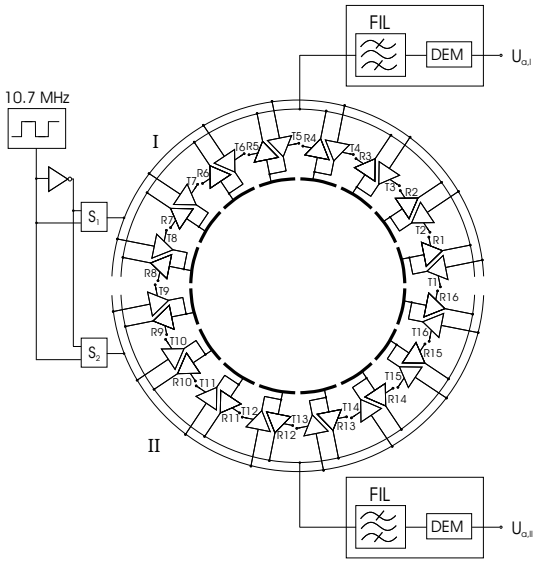

Figure 3: Sensor electronics with tristate amplifiers to switch electrodes between transmitting and receiving state. The circuitry board is split in two half-planes for easier assembly.

regularization parameter is given by

$$\alpha_t = K \frac{\|V_m - V_0\|_2^2}{\|L\varepsilon_r\|_2^2}, \qquad (2)$$

where ε_r is the relative permittivity, which is searched for and K is a constant that has to be found for several test distributions (in our case $K = 10^{-3}$). It is obvious from (2) that the regularization parameter decreases during iterations, since the solution norm $\|V_m - V_0\|_2^2$ decreases, and hence less emphasis is put on the regularization term, bearing the possibility that sharp edges can be reconstructed as well.

The solution of (1) can be found, in principle, with any optimization technique. The most common approach, however, since (1) is from its nature a least squares problem, is a Gauss-Newton scheme, with the principal drawback of large memory requirement for the storage of the approximated Hessian matrix.

A nonlinear conjugate gradient method, on the other hand, does not need the Hessian matrix at all, and hence, at the first sight may be suited better to capacitance tomography problems, where one has to deal with 200 to several thousands of unknowns.

In the following these two methods will be compared on the basis of tests that have been carried out with the capacitance tomography sensor currently in use in our group, consisting of 16 equally distributed electrodes, which can be switched between active and floating states.

ITERATIVE METHODS

The nonlinear conjugate gradients algorithm (NCG) is considered to be one of the most efficient minimization algorithms [2]. In contrast to the quasi-Newton-type methods ([3], [4]) which have quadratically increasing memory requirements and computational complexity with the number of parameters n. For large problems, i. e. a large number of degrees of freedom, it often does not pay off to approximate the Hessian. Conjugate gradient methods avoid a direct approximation of the Hessian and therefore are linear in their memory requirements and computational complexity with respect to n. However, in general the search directions will be worse and conjugate gradient methods demand more iterations for convergence than quasi-Newton-type methods. Nevertheless the overall computation time is smaller for large problems, since each iteration suffers from lower computational cost. For our specific reconstruction problem a nonlinear conjugate gradient algorithm is applied which adapts the formulas of the linear CG. To transform the linear CG into the NCG the step size has to be adjusted and the so-called direction calibration parameter β has to be taken into account. To calculate this parameter the Fletcher-Reeves formula was adopted, [7].

$$\beta_i = \frac{||\nabla f(x_i)||_2^2}{||\nabla f(x_{i-1})||_2^2} \qquad (3)$$

where x denotes the nonlinear inverse solution vector and $f(x)$ is the nonlinear error residual. The scalar factor β represents the knowledge carried over from the previous iterations. Thus, the CG method can be seen as a compromise between steepest descent, where no information about previous iterations is exploited, and the quasi-Newton-type methods, where the information about the approximation of the second order derivatives (approximated Hessian) is utilized.

Although the NCG is applicable for reconstructing high contrast permittivity distributions one has to accept the adversarial properties of the algorithm in terms of convergence behavior. In fact convergence problems are occurring if the function to be minimized has many local minima. The convergence properties of CG algorithms and CG re-

lated algorithms are well discussed in several publications, [9], [8].

The Gauss-Newton method is a modification of the general Newton method. The objective function is minimized in a least squares sense. The important feature of this algorithm is that it is possible to calculate the gradient exactly and to approximate the second order derivative matrix with a rather high accuracy. However, the algorithm improves the accuracy of the approximated Hessian successive in each iteration starting with a very bad estimation of the Hessian. The obtained convergence is much more faster than using quasi-Newton-type methods. Since the Gauss-Newton method can suffer from the same problems like any other second derivative method, a line search approach is advisable. However, no matter how the search direction is evaluated, problems occur if the system matrix is ill-conditioned or even singular. The larger the ratio of the largest and smallest singular values of the system matrix is, the slower is the rate of convergence of the algorithm. Due to this common problem, especially in solving inverse problems, regularization has to be introduced. For analyzing the performance of different algorithms the NCG and a Gauss-Newton (GN) based scheme using an approximation of the second derivative matrix are applied to solve the inverse regularized problem. For both methods a line search based on quadratic interpolation is applied. Additionally, an active set strategy to restrict the permittivity values to reasonable values is implemented.

The gradient of (1) required for both methods is given by

$$g_t = 2J_t^T \left(V_{m,t} - V_0\right) + 2\alpha L^T L \varepsilon_{r,t}, \qquad (4)$$

where J is the Jacobian matrix, whose entry in the i^{th} row and j^{th} column equals

$$J_{i,j} = \frac{\partial V_m^i}{\partial \varepsilon_r^j}. \qquad (5)$$

The Jacobian matrix can be calculated most efficiently by means of the adjoint variable method [6].

The update for the relative permittivity vector for iteration $t+1$ is given by

$$\varepsilon_{r,t+1} = \varepsilon_{r,t} + \gamma_t \frac{g_t^T g_t}{g_{t-1}^T g_{t-1}} \varepsilon_{r,t} - g_t \qquad (6)$$

according to Fletcher and Reeves [7] for the NCG and

$$\begin{aligned} \varepsilon_{r,t+1} \quad = \quad & \varepsilon_{r,t} - \gamma_t \left(J_t^T J_t + \alpha_t L^T L\right)^{-1} \\ & \left(J_t^T \left(V_{m,t} - V_0\right) + \alpha_t L^T L \varepsilon_{r,t}\right) \end{aligned} \qquad (7)$$

for the Gauss-Newton method.

In (7) and (6) γ_t is the stepsize at iteration t, which results from a quadratic interpolation based line search.

RECONSTRUCTION RESULTS

For testing the two iterative reconstruction algorithms a test distribution was chosen. In particular, a PVC bar ($\varepsilon_r = 2 - 4$) was positioned in the center of an air-filled tube ($\varepsilon_r = 1$) (fig. 4). Fig. 5 and fig. 6 illustrate the reconstructed test distribution for both GN and NCG method. The behavior of the solution norm and the progression of the regularization parameter is faced in fig. 7 and fig. 8.

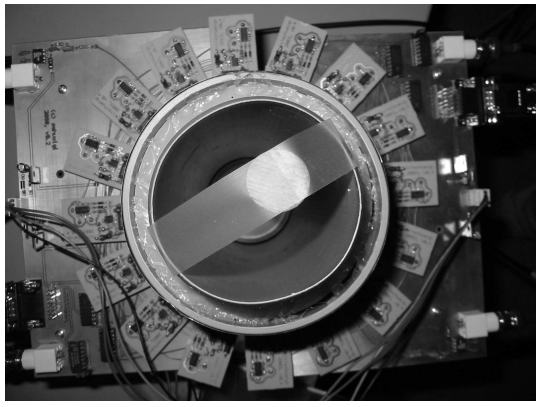

Figure 4: Dielectric cylindrical rod placed near the center of the tube. The electronics for the 16 electrodes can be seen as well.

DISCUSSION

The comparison of fig. 5 and fig. 6 indicate that the Gauss-Newton method performs better than the conjugate gradient method what reconstruction accuracy is concerned. An explanation for this can be found when looking at fig. 7. The solution norm obtained with the conjugate gradient method does not decline to the value for this norm obtained with the Gauss-Newton method (even for 150 iterations) indicating that the NCG got stuck in some suboptimal minimum.

The progression of the regularization parameter (which has been calculated with (2)) shows de-

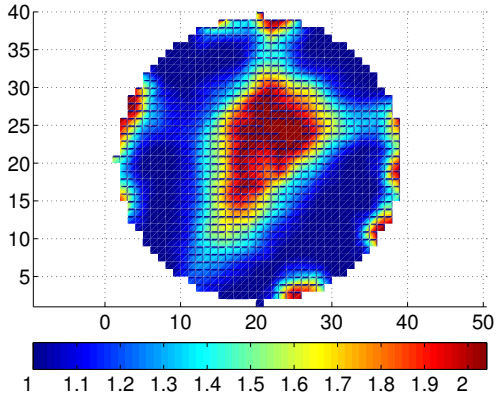

Figure 5: Reconstructed distributions with adapted regularization parameter using Gauss-Newton method. The GN scheme needs about 20 iterations for a reasonable result.

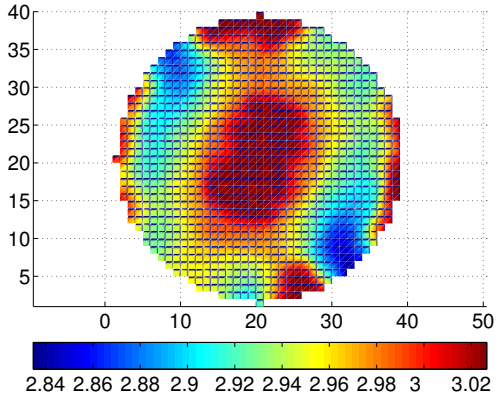

Figure 6: Reconstructed distributions with adapted regularization parameter using conjugate gradient method. The NCG takes about 140 iterations.

creasing behaviour over the iterations, which is immediately clear from (2), since the solution norm decreases as well. Due to the fact that the value of the solution norm is higher in case of the conjugate gradient method, the same must hold for the regularization parameter. The higher values for the regularization parameter reflect in fig. 6, where the permittivity distribution is much more homogeneous than for the Gauss-Newton reconstruction result (note that the discrete Laplacian operator based regularization term penalizes non-smooth material distributions).

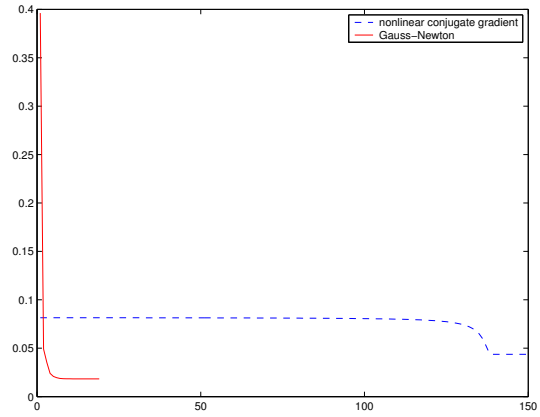

Figure 7: Progression of the solution norm $\|V_{calc} - V_{meas}\|_2^2$.

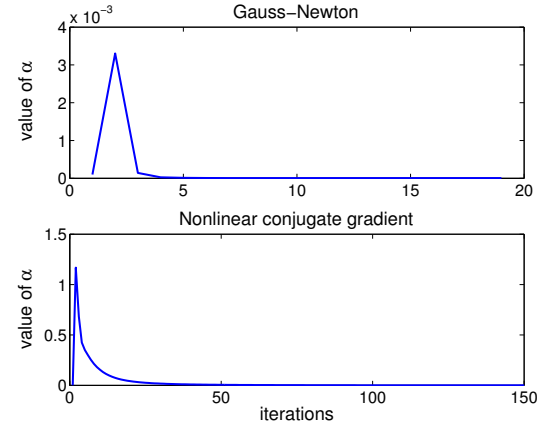

Figure 8: Progression of the regularization parameter α over iterations of reconstruction for GN and NCG method. The difference in the magnitude of the adapted parameter is significantly.

CONCLUDING REMARKS

An analysis of the performance of the two described iterative algorithms for our image reconstruction problem based on real measurement data was given. Even though for the NCG less matrix vector operations have to be performed, and hence this method needs less computation time for one iteration than the Gauss-Newton method, NCG can not compete with the Gauss-Newton method, what accuracy and number of iterations is concerned.

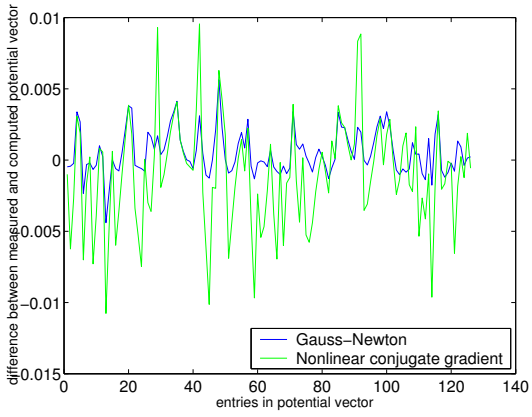

Figure 9: Remaining error between the measured potential vector and the computed potential vector. The fitting between measurement model and mathematical model can be improved using the Gauss-Newton scheme instead of nonlinear conjugate gradient method.

REFERENCES

[1] B. Brandstätter, G. Holler, D. Watzenig, "Reconstruction of inhomogeneities in fluids by means of capacitance tomography", *International Journal for Computation and Mathematics in Electrical and Electronic Engineering (COMPEL)*, vol. 22, no. 3, pp. 508-519, 2003.

[2] S. G. Nash, A. Sofer, *Linear and nonlinear Programming*, McGraw-Hill International Editions, New York, 1996.

[3] N. Polydorides, W. R. B. Lionheart, H. McCann, "Krylov subspace iterative techniques: on the detection of brain activity with electrical impedance tomography", *IEEE Transactions on Medical Imaging*, vol. 21, issue 6, pp. 596 - 603, 2002.

[4] C. R. Vogel, *Computational Methods for inverse Problems*, SIAM, Philadelphia, USA, 2002.

[5] D. Watzenig, B. Brandstätter and G. Holler, 'A Condition-Number Based Regularization Parameter Estimate for Reconstruction Problems, *in print for IEEE Transactions on Magnetics, 2004*

[6] B. Brandstätter and B. Kortschak, 'A Comparison of the Mutual Energy Concept with an Adjoint State Approach for Jacobian Calculation in ECT', *Proceedings of the 3rd World Congress on Industrial Process Tomography*, Banff, Alberta, Canada, September 2-5, 2003, pp. 397-402.

[7] R. Fletcher and C. M. Reeves, 'Function minimization by conjugate gradients', *Computer J.*, vol. 7, pp. 149-154

[8] G. H. Golub and C. F. van Loan, *Matrix computations*, 3rd edition, Johns Hopkins University Press, Baltimore, 1996.

[9] M. Hanke, "Conjugate gradient type methods for ill-posed problems",Scientific and Technical, Longman, Essex, 1995.